Displacement-Based Seismic Design for Reinforced Masonry Shear-Wall Structures, Part 1: Background and Trial Application

Farhad Ahmadi,[a] Marios Mavros,[b] Richard E. Klingner,[c] Benson Shing,[d] and David McLean[e]

In this paper, a displacement-based seismic design procedure is presented for reinforced masonry shear-wall structures, with the objective of being more consistent, transparent, and practical than current force-based seismic design procedures. The procedure anticipates the formation of a plastic mechanism at specified target displacements, calculates the local deformation demands associated with that mechanism, and ensures that those local deformation demands remain below deformation capacities for flexure-dominated and shear-dominated wall segments. Guidelines to determine the target displacements and effective damping properties for reinforced masonry wall structures are provided. The proposed procedure and guidelines are used in a trial application to design a full-scale, two-story reinforced masonry shear-wall system. [DOI: 10.1193/120212EQS344M]

INTRODUCTION

In the last decade, a number of seismic design approaches have been developed, with the goal of limiting the global and local deformations of a structure to acceptable levels under design earthquakes (Priestley et al. 2007). These approaches are more rational than purely force-based design methods, because they consider the fact that damage is related directly to the inelastic deformation of a structure. One such approach is the direct displacement-based seismic design method as presented in Priestley et al. (2007). With this method, the designer designs the building so that its maximum displacement under a specified design earthquake satisfies its deformation capacity, which can be determined from the structural material, structural configuration, and anticipated member detailing.

This paper discusses the need for and the advantages of displacement-based seismic design for reinforced masonry buildings, most of which are low-rise structures, and presents a trial application of the method to a full-scale, shear-controlled, two-story reinforced

[a] Postdoctoral Research Associate, Dept. of Civil Engineering, The University of Texas at Austin, 1 University Station C1700, Austin, TX 78712
[b] Graduate Research Assistant, Dept. of Structural Engineering, University of California, San Diego, 9500 Gilman Dr., La Jolla, CA 92093
[c] L. P. Gilvin Professor in Civil Engineering, The University of Texas at Austin, 1 University Station C1700, Austin, TX 78712
[d] Professor, Dept. of Structural Engineering, University of California, San Diego, 9500 Gilman Dr., La Jolla, CA 92093
[e] Professor, Dept. of Civil Engineering, Washington State University, 405 Spokane Street, Sloan 101, Pullman, WA 99164

Earthquake Spectra, Volume 31, No. 2, pages 969–998, May 2015; © 2015, Earthquake Engineering Research Institute

masonry shear-wall system, for which the use of a force-based design approach would not be rational. This study is part of a bigger research project aimed at improving performance-based design methodologies for fully grouted, reinforced masonry structures. The displacement-based design procedure presented here is supported by extensive quasi-static and shake-table test data generated in this project (Ahmadi 2012, Sherman 2011, Stavridis et al. 2012), and by a computational model developed and validated using the test data. The ability of the structure designed in the trial application to meet the performance objectives has been evaluated with data from shake-table tests as presented in a companion paper (Ahmadi et al. 2013).

LIMITATIONS OF FORCE-BASED SEISMIC DESIGN FOR REINFORCED MASONRY SHEAR-WALL STRUCTURES

Current seismic design provisions in the United States (ASCE/SEI 7-10) use force-based design for structures, including reinforced masonry structures. The design method in ASCE/SEI 7-10 first prescribes seismic design loads in terms of a building's geographic location, its function, and the characteristics of the underlying soil. These three descriptors define the building's seismic design category (SDC). That SDC corresponds to a list of permitted structural systems such as shear wall types, each of which is to be designed with a designated force-reduction factor, R, representing a combination of probable system ductility and system over-strength. Masonry buildings in seismic design categories D and higher are required to have seismic force-resisting systems composed of so-called special reinforced masonry shear walls. Based on the initial elastic period of the structure (including the effects of flexural cracking in wall sections) and the elastic design response spectrum for the given site reduced by the R-factor, the design base shear force is calculated and is distributed among masonry shear-wall segments according to their relative stiffnesses. Each masonry shear-wall segment must be provided with sufficient flexural (longitudinal) reinforcement to resist its factored design moments and axial forces, and sufficient transverse reinforcement to resist its factored design shears. Segments of "special" reinforced masonry shear walls also must be designed for the shears that could be demanded by possible flexural overstrengths in the segments. Finally, each segment must meet prescriptive requirements for the minimum percentages and the maximum spacing of reinforcement. After wall segments are designed, inelastic displacements are calculated as the elastic displacements (considering cracked sections) due to the design seismic force multiplied by the displacement amplification factor (C_d). The resulting inelastic displacements must meet code limits.

Although forced-based design has proven generally safe in past earthquake events, it has the following limitations for typical reinforced masonry buildings:

1. Force-based seismic design does not explicitly recognize deformation-related limit states. As shown in Figure 1, damage is directly related to inelastic deformations, not to forces. This design method does not ignore deformations entirely, however, because the design lateral forces are limited through the R-factor, which depends on the available ductility of the structural system.
2. The assumed independence of the R-factor on the structural period is inherently inconsistent with the actual inelastic response of structures, particularly for short-period structures (Miranda and Bertero 1994). As a result, this design

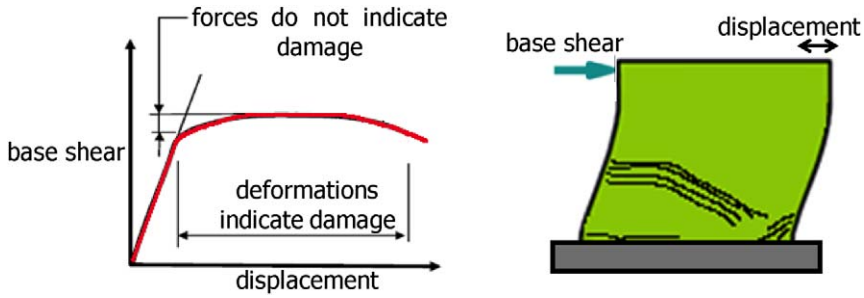

Figure 1. Schematic load-displacement curve and associated damage.

approach may not produce consistent structural behavior. The same can be said for the assumed independence of the system overstrength factor on the actual structural configuration.

3. The justification for tying seismic design factors (*R*, displacement amplification, and overstrength factors) to seismic design categories is not clear. While some inelastic deformation capacity is required to reduce the probability of collapse under extreme ground motions, arbitrarily high levels of ductility (such as a required *R*-factor of 5 for the "special" reinforced masonry shear walls required in SDC D and higher) are not necessary. Post-earthquake reconnaissance studies of modern reinforced masonry buildings show that these buildings are much stronger and ductility demands are much lower than commonly assumed in design (Klingner 1994). In fact, modern reinforced masonry buildings with high plan densities of walls can successfully resist seismic forces consistent with lower *R*-factors.
4. Current force-based seismic design codes (ASCE/SEI 7-10 and the 2011 MSJC *Code*) do not control the aspect ratios of walls or wall segments. As a result, for example, it is perfectly possible for a code-compliant "special" reinforced masonry shear wall to be incapable of ductile behavior.
5. Force-based design uses technically questionable requirements for prescriptive reinforcement. Current MSJC prescriptive reinforcement requirements for special reinforced masonry shear walls can provide ductility where it is not required, and can provide insufficient ductility where it is actually required. Ductile detailing should be required only in wall segments where inelastic deformations are expected, such as plastic hinge zones.
6. Force-based seismic design is not logical for perforated walls. The overall behavior of a perforated wall building cannot easily be classified as ductile or non-ductile because of different behaviors and contributions of its component wall segments.

DISPLACEMENT-BASED DESIGN FOR REINFORCED MASONRY

Displacement-based design was first introduced in the 1990s, and has been applied to different structural systems (Moehle 1992, Priestley 1997, Munshi and Ghosh 2000, Filiatrault and Folz 2002). A methodology for displacement based seismic design of wall structures was proposed by Sullivan et al. (2006). Although some recently proposed

displacement-based procedures specifically address masonry structures (Calvi 1999), they are not sufficiently specific and have not yet been sufficiently validated. The procedure adopted here follows the work of Filiatrault and Folz (2002) and Priestley et al. (2007), but is specifically tailored to fully grouted reinforced masonry structures using the experimental data obtained in this research. The key steps of that procedure are shown in Figure 2 and discussed below.

STEP 1: DEFINE SEISMIC HAZARD

Seismic hazard levels for the design of new structures have traditionally been a design earthquake (DE; formerly referred to as a design basis earthquake, or DBE) with a probability

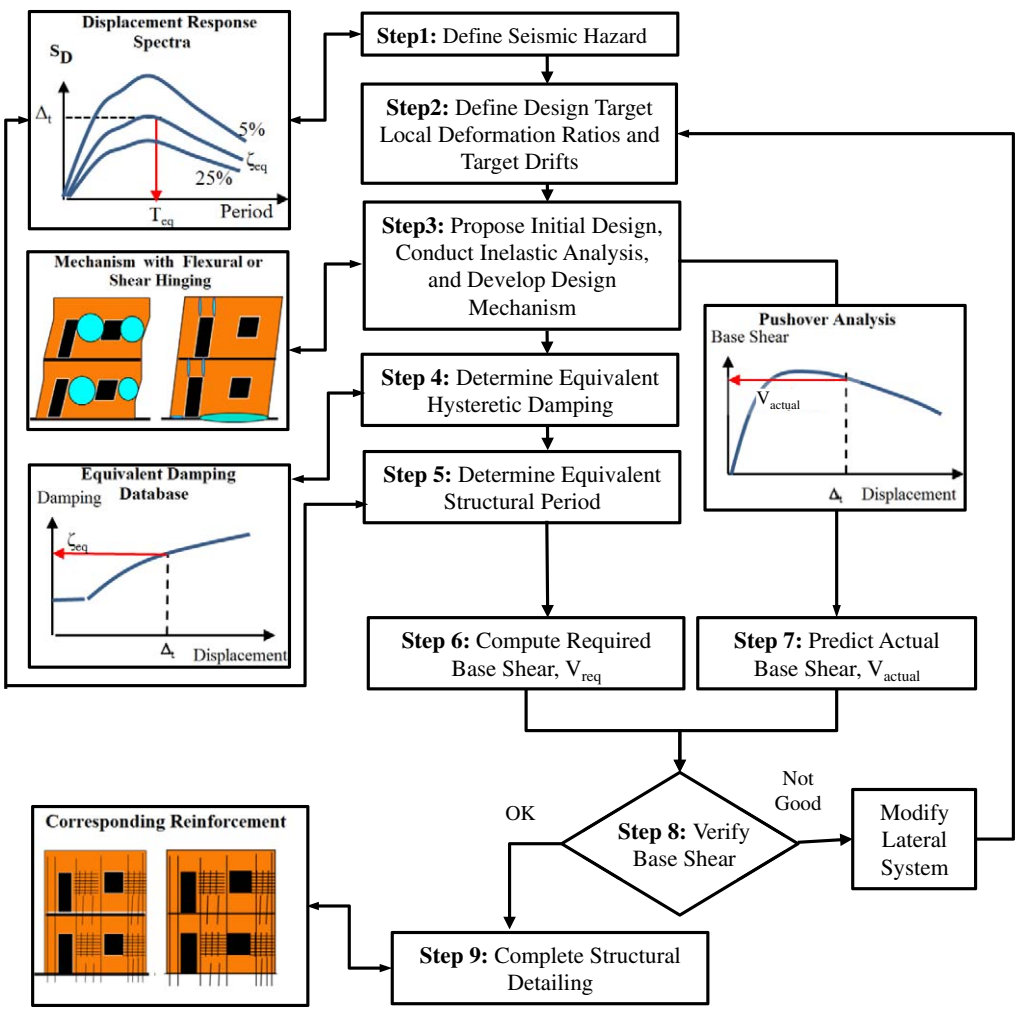

Figure 2. Modified flowchart of displacement-based design method for reinforced masonry shear-wall structures.

of exceedance of 10% in 50 years, and a maximum considered earthquake (MCE), with a probability of exceedance of 2% in 50 years. Although in ASCE7-10 these traditional definitions are modified to produce "risk-targeted" ground motions with uniform probabilities of collapse, rather than uniform probabilities of exceedance, the basic principle remains essentially the same. In this work, these seismic hazard levels are considered. For the purpose of displacement-based design, the code design spectral accelerations, S_a, for a given seismic design category can be transformed into corresponding spectral displacement values S_D.

$$S_D = \frac{T_{eq}^2}{4\pi^2} S_a \tag{1}$$

where T_{eq} is the equivalent elastic period of the building at the target displacement level (or local deformation limits). Spectral accelerations given in design codes typically correspond to equivalent viscous damping equal to 5% of critical. For displacement-based design, these values have to be modified to account for the effects of hysteretic energy dissipation. The spectral displacement, $S_{D-\xi_{eq}}$, corresponding to the total equivalent viscous damping, ξ_{eq}, of the structure including inelastic response, can be obtained through empirical modification factors such as that given in Equation 2 (Filiatrault and Folz 2002), which had been previously adopted in Eurocode 8 (1998). The determination of ξ_{eq} for reinforced masonry shear-wall structures is discussed later in this paper.

$$S_{D-\xi_{eq}} = \sqrt{\frac{0.07}{0.02 + \xi_{eq}}} S_D \tag{2}$$

STEP 2: DEFINE DESIGN TARGET DRIFT LIMITS OF WALL SEGMENTS AND TARGET DISPLACEMENTS

To assure the good performance of a structure, the story drift ratios (relative lateral displacements between floors divided by story heights) for the specified earthquake hazard levels (DE and MCE) must not exceed the target story drift ratios of the structure, which can be established based on the local deformation capacity limits of the wall segments comprising the structure. The latter can be obtained from experimental data. As part of this project, 41 reinforced masonry shear-wall specimens were tested under reversed cyclic loading at The University of Texas at Austin (UT Austin) and at Washington State University (WSU). The specimens had different types of detailing, axial load, aspect ratio, and boundary conditions (Sherman 2011, Ahmadi 2012). Most of them were flexure-controlled, and some were shear-controlled. Data from those wall specimens are used here to determine the deformation limits of wall segments for DE and MCE hazard levels, considering reasonable strength loss and damage for each level. The limiting deformation ratios (relative displacements between the top and bottom of wall components divided heights) determined for different categories of wall segments are summarized in Table 1. For this purpose, flexure-controlled wall segments are subdivided into three categories; one for walls with high aspect ratios (4.0 and higher), another for walls with intermediate aspect ratios (between 1.0 and 4.0), and still another for walls with low aspect ratios (1.0 and lower). Most but not all flexure-controlled wall segments met prescriptive requirements for special reinforced masonry shear walls.

Table 1. Local deformation ratio limits for reinforced masonry shear wall segments

	Aspect ratio	Local deformation ratio limits	
		Design earthquake (DE)	Maximum considered earthquake (MCE)
Flexure-controlled wall segments	4 and higher	1.50%	2.50%
	between 1.0 and 4.0	1.20%	2.00%
	1.0 and lower	0.80%	1.50%
Shear-controlled wall segments	All cases	0.50%	1.00%

Typical load-displacement loops for flexure-controlled wall segments with different aspect ratios, tested under reversed loading at UT Austin and Washington State University, are shown in Figure 3. Proposed deformation limits for each aspect ratio are also shown in the plots.

Typical load-displacement loops for shear-controlled wall segments tested under reversed loading at UT Austin are shown in Figure 4, along with the proposed deformation limits. The proposed deformation limits depend on shear reinforcement, and the percentages of shear reinforcement selected for testing satisfy current MSJC (2011) requirements for special reinforced masonry shear walls or draft 2013 MSJC requirements for shear hinging regions. Those local deformation limits, converted to story drift limits using the relationship between wall segment heights and story heights, are consistent with the story drift limits observed by Stavridis et al. (2012) in the shake-table tests of a three-story, full-scale specimen, conducted as part of this project.

Given the local deformation limits of wall segments, and knowing the relationship between wall segment heights and story heights, the target story drift limits and the corresponding target displacements of a structure can be established. The local deformation limits of wall segments depend on whether those segments are flexure- or shear-controlled. This can often be determined from the geometric configuration of the wall system (which determines the effective aspect ratios of wall segments between window and door openings), and from the reinforcing details of the wall segments.

STEP 3: PROPOSE INITIAL DESIGN AND CONDUCT INELASTIC ANALYSIS

To determine the target displacements for the structure, an initial wall configuration with a preliminary reinforcing scheme is needed. This can be developed based on an initial elastic analysis, out-of-plane design actions, experience, or other means. This point is discussed further in the specific design example presented later in this paper. Once the design seismic hazard and associated target displacements have been defined and a preliminary design has been developed, a nonlinear pushover analysis can be conducted to determine the probable inelastic mechanism of the system and the controlling failure modes that can be developed in

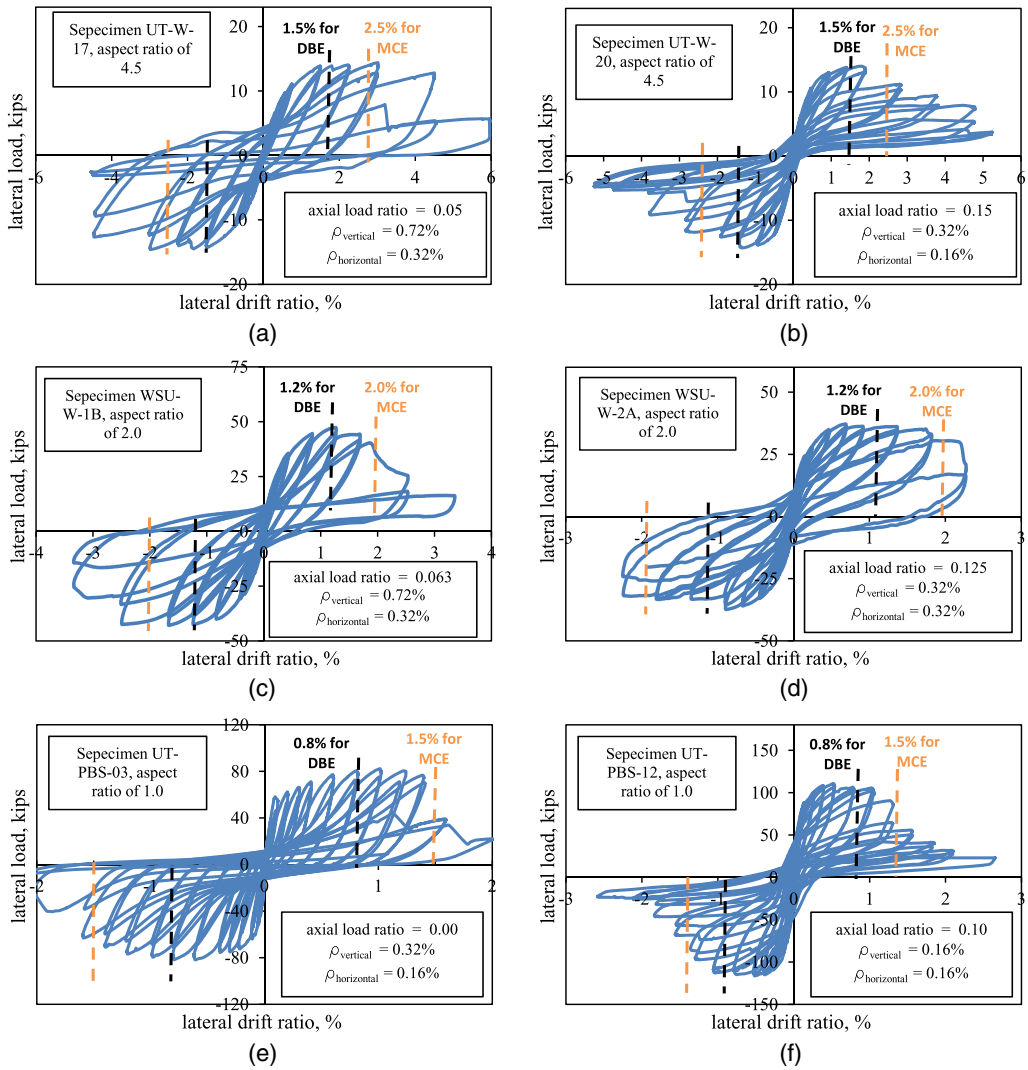

Figure 3. Typical lateral load-displacement loops for flexure-controlled reinforced masonry wall segments with aspect ratios of 4.5, 2.0, and 1.0 ($\rho_{vertical}$ and $\rho_{horizontal}$ correspond to the vertical and horizontal reinforcement ratios, respectively).

critical wall segments. Based on this analysis, the reinforcing details can be modified as necessary to achieve the desired or intended inelastic mechanism, or the target displacements can be revised to be consistent with the mechanism expected from the analysis. Once these tasks have been accomplished, an equivalent single-degree-of-freedom (SDOF) system is determined, to which displacement-based design can be applied. Procedures for doing this have been proposed by Calvi and Kingsley (1995), Priestley et al. (2007), and Mehrabi and Shing (2003). These methods require an inelastic pushover analysis to determine the

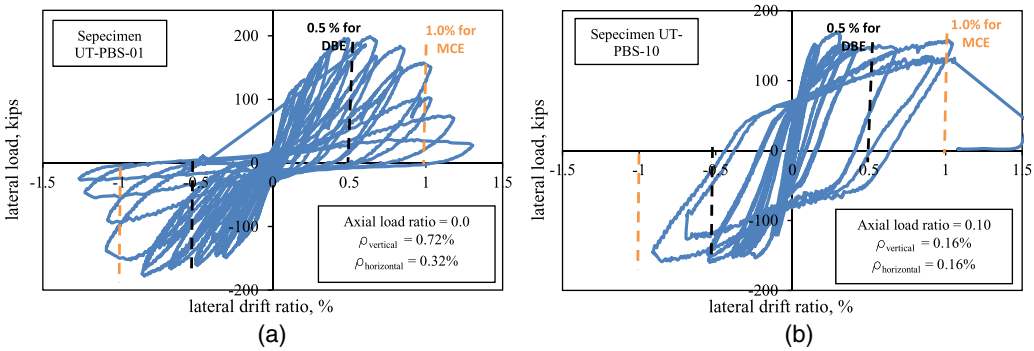

Figure 4. Typical lateral load-displacement loops for shear-controlled reinforced masonry wall segments ($\rho_{vertical}$ and $\rho_{horizontal}$ correspond to vertical and horizontal reinforcement ratios, respectively).

likely deflected shape of the structure when the target displacements have been reached. With this information, a target displacement can then be determined for the equivalent SDOF system. According to the method proposed by Calvi and Kingsley (1995) and recommended by Priestley et al. (2007), the equivalent target displacement, Δ_{eq}, and the effective seismic weight, W_{eff}, for the equivalent SDOF system are given by Equations 3 and 4.

$$\Delta_{eq} = \frac{\sum W_i u_i^2}{\sum W_i u_i} \tag{3}$$

$$W_{eff} = \frac{(\sum W_i u_i)^2}{\sum W_i u_i^2} \tag{4}$$

where W_i and u_i are the seismic weight and the target displacement at level i of the original multi-story structure.

STEP 4: DETERMINE EQUIVALENT HYSTERETIC DAMPING

The hysteretic energy–dissipation characteristics of the structure at the target displacement can be expressed in terms of an equivalent viscous damping ratio ξ_{eq}. For this purpose, a database for equivalent viscous damping must be established for reinforced masonry wall systems. Equivalent viscous damping at a displacement amplitude Δ_t can be estimated from the hysteretic load-displacement curves of the structural components using Equation 5 (Filiatrault and Folz 2002; Priestley et al. 2007).

$$\xi_{eq} = \frac{E_{D\Delta_t}}{2\pi k_{eq}\Delta_t^2} + \xi_0 \tag{5}$$

where $E_{D\Delta t}$ is the hysteretic energy dissipated per cycle with a displacement amplitude Δ_t, which corresponds to the target displacement, and k_{eq} is the equivalent lateral secant stiffness of the building at that displacement. The nominal viscous damping ratio, ξ_0, accounts for the

elastic energy–dissipation characteristics of other structural and nonstructural elements, and can be reasonably taken as 5% of critical (Priestley et al. 2007). Applying Equation 5 to the results of reversed cyclic testing from this research project, equivalent viscous damping ratios for flexure-controlled reinforced masonry wall segments with two different aspect ratios, and also for shear-controlled reinforced masonry wall segments have been calculated and expressed as functions of the drift ratio, as presented in Figure 5. For flexure-controlled wall segments with aspect ratios between 1.0 and 2.0, the damping ratio used for design can be obtained by linear interpolation between the values for an aspect ratio of 1.0 and an aspect ratio of 2.0. Based on the target drift limits, the equivalent viscous damping for each wall segment for each seismic hazard level can then be determined using the appropriate plot(s) in Figure 5.

With multiple in-plane walls, effective global damping may be calculated as a weighted average based on the distribution of shear forces among the wall elements as shown in Equation 6 (Priestley et al. 2007).

$$(\xi_{eq})_{global} = \frac{\sum(V_i \xi_{eq-i})}{\sum V_i} \tag{6}$$

In this equation, V_i and ξ_{eq-i} are the shear force and the equivalent damping, respectively, in the ith wall segment at the target displacement. Assuming that the base shear is distributed

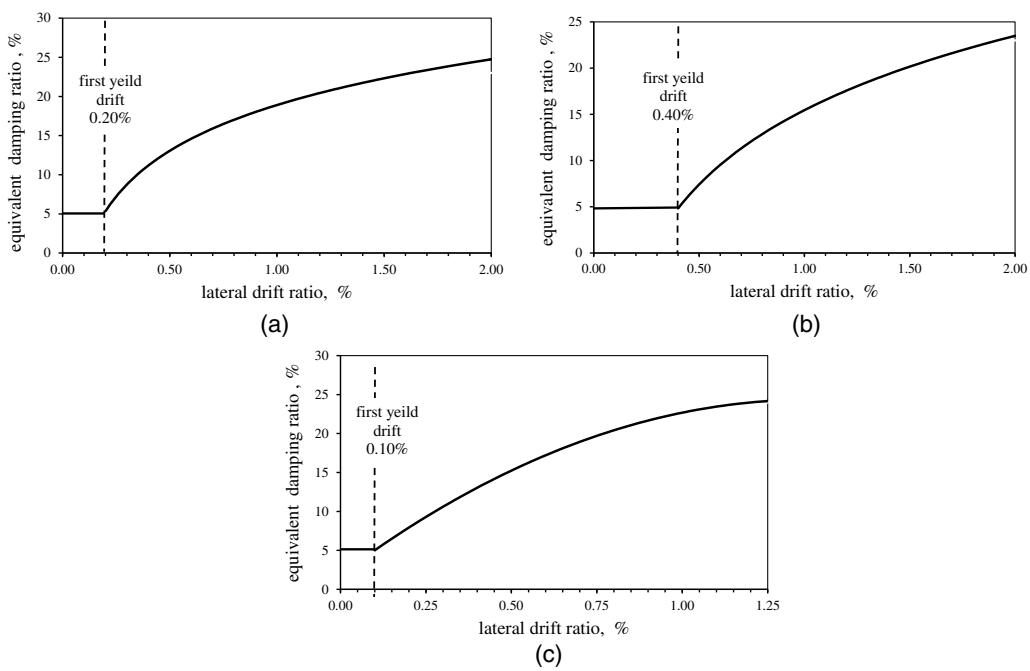

Figure 5. Equivalent viscous damping for reinforced masonry wall segments: (a) flexure-controlled walls with aspect ratios of 1.0 and lower; (b) flexure-controlled walls with aspect ratios of 2.0 and higher; (c) shear-controlled walls.

among walls in proportion to the square of the plan length, l_{wi}, of each wall segment i, Equation 6 can be rewritten as Equation 7.

$$(\xi_{eq})_{global} = \frac{\sum (i_{wi}{}^2 \xi_{eq-i})}{\sum l_{wi}{}^2} \tag{7}$$

STEP 5: DETERMINE EQUIVALENT STRUCTURAL PERIOD

Knowing the target displacement for the equivalent SDOF system and the global equivalent viscous damping (including inelastic effects) $(\xi_{eq})_{global}$ of the building at that target displacement, the equivalent elastic period of the building, T_{eq}, can be obtained directly from the displacement response spectrum at the selected hazard level.

STEP 6: COMPUTE REQUIRED BASE SHEAR

Representing the building as an equivalent linear SDOF system with known effective weight W_{eff} and structural period T_{eq}, the required equivalent lateral stiffness $(k_{eq})_{req}$ can be obtained using Equation 8:

$$(k_{eq})_{req} = \frac{4\pi^2 W_{eff}}{g T_{eq}^2} \tag{8}$$

in which g is the acceleration due to gravity. The effective weight depends on the inelastic deflected shape for the structure at the target displacement, as shown in Equation 4. In this step, the required base shear capacity V_{req} of the building can be calculated using Equation 9 for Design and MCE levels.

$$V_{req} = (k_{eq})_{req} \Delta_{eq} \tag{9}$$

STEP 7: PREDICT BASE SHEAR CAPACITY

For each hazard level, the base shear capacity of the building V_{actual} at the target displacement Δ_t, can be obtained from the static pushover analysis conducted in Step 3.

STEP 8: VERIFY BASE SHEAR

The predicted base shear capacity of the building is compared to the required base shear. If these values differ substantially or if the predicted base shear capacity is lower than that required, the design should be modified. If the predicted based shear capacity is a little higher than that required, then the design is satisfactory. The design can then be checked by nonlinear time-history analysis using a few ground-motion records with characteristics representative of the site to make sure that the structural displacements are within the target limits.

STEP 9: COMPLETE STRUCTURAL DETAILING

Using the local deformation demands, the initial detailing of the wall segments and other elements is refined as necessary for sufficient inelastic shearing deformation capacity in

shear hinging regions, and for sufficient inelastic rotation capacity in flexural hinging regions. The required base shear capacity of the building that has been computed at the target displacement (Equation 9) is then used to design the structural elements that are intended to behave elastically. These elements must be provided with sufficient strength to resist the required actions.

DEVELOPMENT AND VERIFICATION OF ANALYTICAL TOOLS

Prediction of the nonlinear response of reinforced masonry structures is fundamental to their displacement-based design. In this paper, "General Wall Elements," macro elements implemented in PERFORM-3D (CSI 2007), have been used for response prediction. They have been calibrated for reinforced masonry shear-wall structures using results of reversed cyclic loading tests on reinforced masonry shear walls, as presented in a previous section, and using a full-scale, three-story specimen tested on a shake-table (Stavridis et al. 2012). Each General Wall Element has 4 nodes and 24 nodal degrees of freedom. Of those 24 degrees of freedom, eight are associated with in-plane displacements of the element. To model bending, shear and diagonal compression behavior, the "General Wall Element" consists of five layers acting in parallel. These layers are shown in Figure 6 (CSI 2007). In this study, only the vertical and horizontal axial/bending layers and the shear layer are used. Each of the axial/bending layers, as shown in Figure 6a and Figure 6b, is composed of nonlinear fibers. The shear layer, shown in Figure 6c, has a uniform shear strain, a uniform thickness, and a nonlinear relationship between shear stress and shear strain. Each layer behaves independently; however, the layers interact because they are connected at the nodes; and their combined behavior defines the behavior of the General Wall Element. For modeling most walls, it is customary to ignore the diagonal layers, and to use only the two bending layers and the shear layer (CSI 2007).

When masonry or concrete is subjected to combined compression and shear, their shear strength is increased, essentially because of the change of the stress state and enhanced aggregate interlock forces. The General Wall Element does not account for these. The shear strength in the shear layer is assumed to be independent of other stresses. Another principal simplification of the General Wall Element is that each fiber in an axial/bending layer has a uniform axial strain, and each shear layer has a uniform shear strain. Hence, the curvature and, therefore, the moment developed in an axial/bending layer is uniform along the direction of the fibers. This results in a lower-order element than a typical beam element, in which curvature is assumed to vary linearly along the element length. Nevertheless, with the

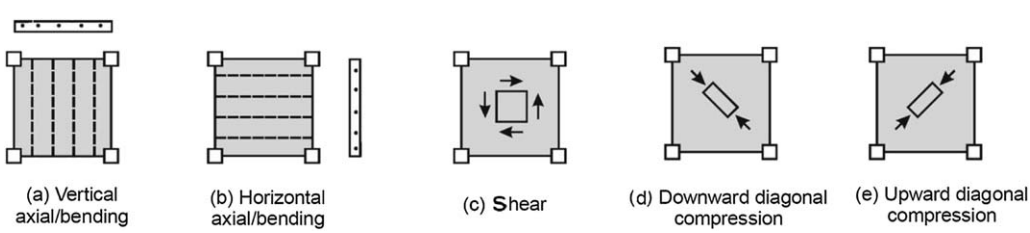

Figure 6. Parallel layers comprising the General Wall Element (CSI 2007).

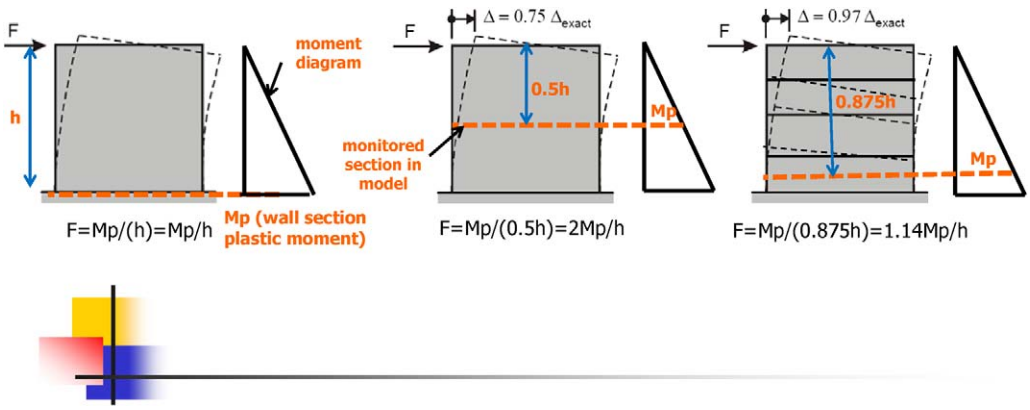

Figure 7. Error in flexural strength resulting from the superposition of bending and shear layers in the General Wall Element of PERFORM-3D (CSI 2007). (a) Exact strength; (b) model with single element; (c) model with four elements.

superposition of a shear layer, a linear moment gradient is introduced along the length of an element with the moment at the mid-height or mid-length of the element equal to that calculated with the fiber section. This will lead to a significant over-estimation of the moment capacity of a wall if the element height is significant compared to the wall height as illustrated in Figure 7. As shown in Figure 7a, moments in the real wall increase linearly from tip to base, and the wall yields when the moment at the base reaches the wall's yield capacity. As shown in Figure 7b, if the wall segment is modeled with a single element extending the entire wall height, the moment at the base of the wall will be twice as large as the actual moment capacity when the moment at the mid-height of the wall reaches the moment capacity of the fiber section. As shown in Figure 7c, this error can be reduced by increasing the number of elements used over the height of a wall. With four elements, capacity is over-estimated by a factor of 1.14. To address this issue and have an accurate assessment of the moment capacity of a wall, the height of the General Wall Elements in the plastic hinge zone should be small compared to the height of the wall. In general, small element sizes can lead to unrealistic strain localization. This can be avoided by having the height or length of the General Wall Elements in a plastic-hinge region comparable to the expected effective plastic-hinge length. This condition was satisfied for the models developed here.

VERIFICATION OF MODELS USING EXPERIMENTAL RESULTS FROM REINFORCED MASONRY SHEAR-WALL SPECIMENS

The accuracy of PERFORM-3D's General Wall Element for predicting the inelastic response of reinforced masonry shear wall segments was investigated by comparing the predicted and measured responses of representative reinforced masonry shear-wall specimens tested under reversed cyclic load at UT Austin and at Washington State University (Ahmadi 2012, Sherman 2011). As shown in Table 2, specimens used in this verification had four different aspect ratios (1.0, 2.0, 3.0, and 4.5).

Table 2. Cantilever wall specimens used to verify and calibrate the general wall element

Specimen	Nominal length, in.	Nominal height, in.	Aspect ratio	Axial load ratio	Vertical reinforcement	Horizontal reinforcement
UT-PBS-03	96	96	1	0	No. 4 at 8 in.	No. 4 at 8 in.
WSU-W-1A	40	80	2	0.0625	No. 6 at 8 in.	No. 4 at 8 in.
UT-W-13	48	144	3	0.05	No. 6 at 8 in.	No. 4 at 16 in.
UT-W-17	32	144	4.5	0.05	No. 6 at 8 in.	No. 4 at 8 in.

To model the strain demand at the base of the walls realistically, the wall specimens were modeled using 8- × 8-in. General Wall Elements. In wall cross-sections modeled using vertical fibers, masonry crushed fiber by fiber in a discrete fashion. The depth of crushing was estimated for each wall segment, and a sufficient number of masonry fibers were placed in that depth.

The vertical and horizontal fibers were modeled using uniaxial material laws calibrated for reinforcement and masonry as shown in Figure 8. The elastic modulus, tensile yield, and ultimate strength of the reinforcing steel were based on the results of material tests. The tensile strength of masonry was neglected, and the compressive behavior was based on the results of monotonic stress-strain tests of CMU (Concrete Masonry Unit) prisms of shear-wall specimens and full-scale shake table specimens. For cyclic loading and dynamic time-history analyses, hysteretic energy dissipation and strength degradation are important parameters, and they were accounted for by specifying hysteretic degradation factors in the material models, as shown in Figure 9. These factors control the reduction in swept area between the original hysteretic loop and the degraded loop, and the changes in the shape of the loops, including pinching (CSI 2007).

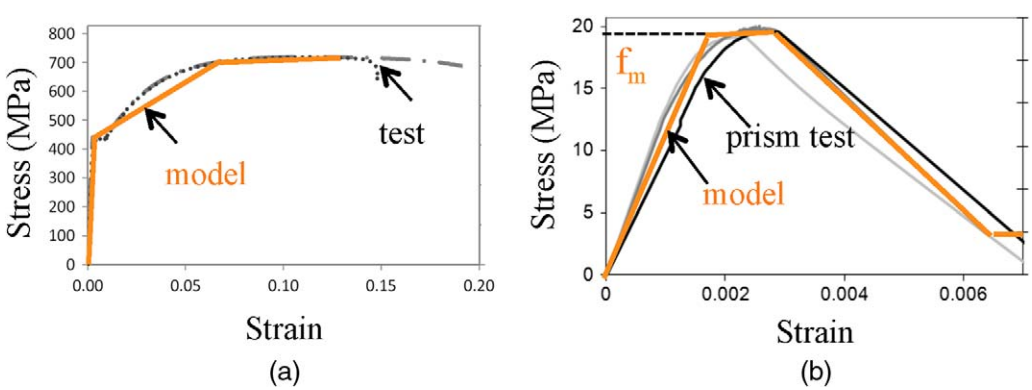

Figure 8. (a) Typical steel stress-strain relation, and (b) typical masonry stress-strain relation used to model reinforced masonry shear walls.

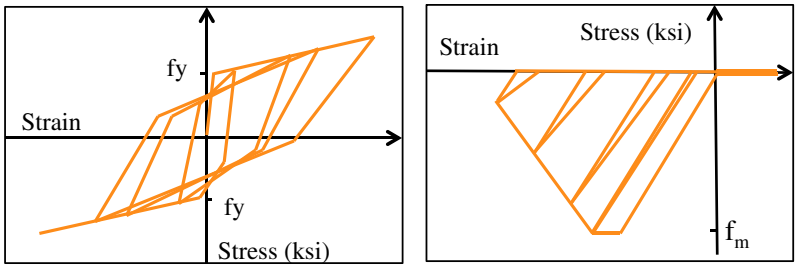

Figure 9. Typical degradation models used in (a) modeling reinforcement and (b) masonry fibers in reinforced masonry shear walls.

Each analytical model of the reinforced masonry shear wall specimen was subjected to the same displacement history as the corresponding test specimen. Gravity load was first applied, followed by a series of lateral displacement cycles. In Figure 10, predicted and measured hysteretic curves of lateral load versus drift are compared for Specimen UT-PBS-03 (aspect ratio 1.0), Specimen WSU-1A (aspect ratio 2.0), Specimen UT-W-13 (aspect ratio 3.0), and Specimen UT-W-17 (aspect ratio 4.5). As shown in Figure 10, the analytical models provided a very accurate match of the stiffness, strength and yield points of the wall specimens. The analytical models also captured the measured hysteretic behavior of wall segments quite well, including stiffness degradation, hysteretic shape, residual displacements, and pinching.

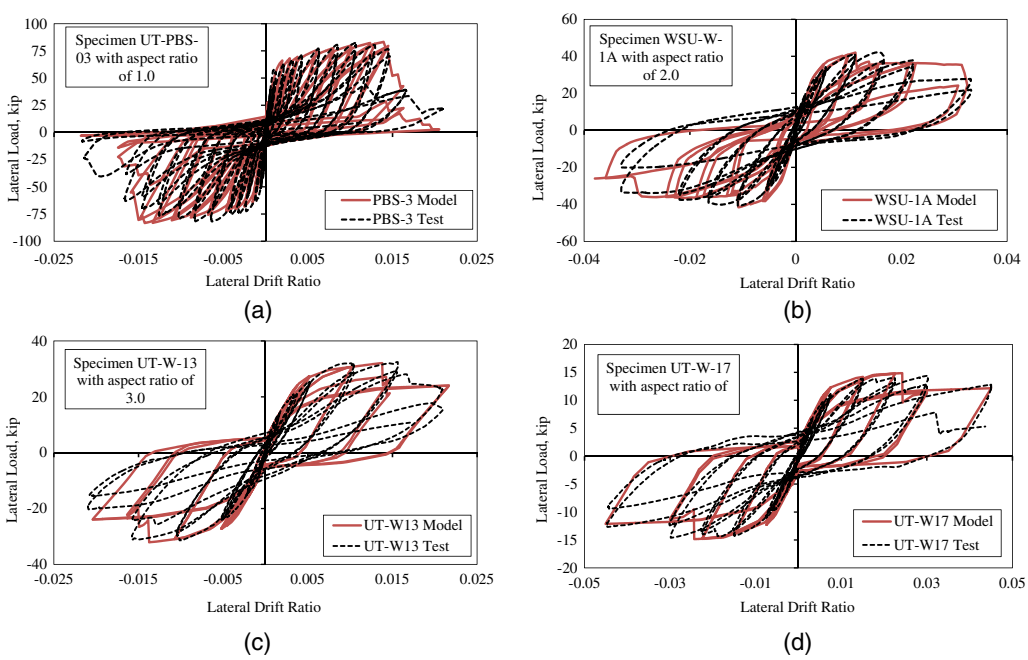

Figure 10. Predicted versus measured load-drift responses for reinforced masonry shear walls.

COMPARISON OF ANALYTICAL PREDICTIONS WITH EXPERIMENTAL RESULTS FOR THREE-STORY SHAKE-TABLE SPECIMEN

In this section, structural response as predicted by the verified "General Wall Element" model is compared with that observed from a three-story reinforced masonry specimen tested on the large high-performance shake table at the University of California, San Diego (Stavridis et al. 2012). The main objectives of shake-table testing were to examine the overall and local behaviors of reinforced concrete masonry buildings designed using force-based procedures, and to use shake-table data from a full-scale structure to extend, refine, and validate analytical models for displacement-based design. The main structural system consisted of two T-walls and one rectangular wall. The floor and roof diaphragms were composed of prestressed concrete hollow-core planks with reinforced concrete topping, which spanned parallel to the direction of shaking. Schematic views of the three-story, full-scale reinforced masonry specimen on the shake table are shown in Figure 11.

As shown in Figure 12, a non-linear model of the three-story specimen were developed using PERFORM-3D (CSI 2007). Nonlinear dynamic analyses were conducted using a set of material parameters selected based on tested material properties, and degradation parameters based on comparisons with the results of reversed cyclic tests. The in-plane wall segments (vertical and horizontal) were modeled with the General Wall Elements. The out-of-plane wall segments were modeled using 3-D inelastic beam-column elements with plastic hinges at each end. The hinges were rigid-plastic, and used yield surfaces calculated based on the nominal capacities given by the MSJC *Code* (2011) provisions to account for axial and bending interaction. The floor slabs were modeled using four-node elastic shell elements with membrane (in-plane) and plate bending (out-of-plane)

Figure 11. Schematic views of three-story, full-scale reinforced masonry specimen.

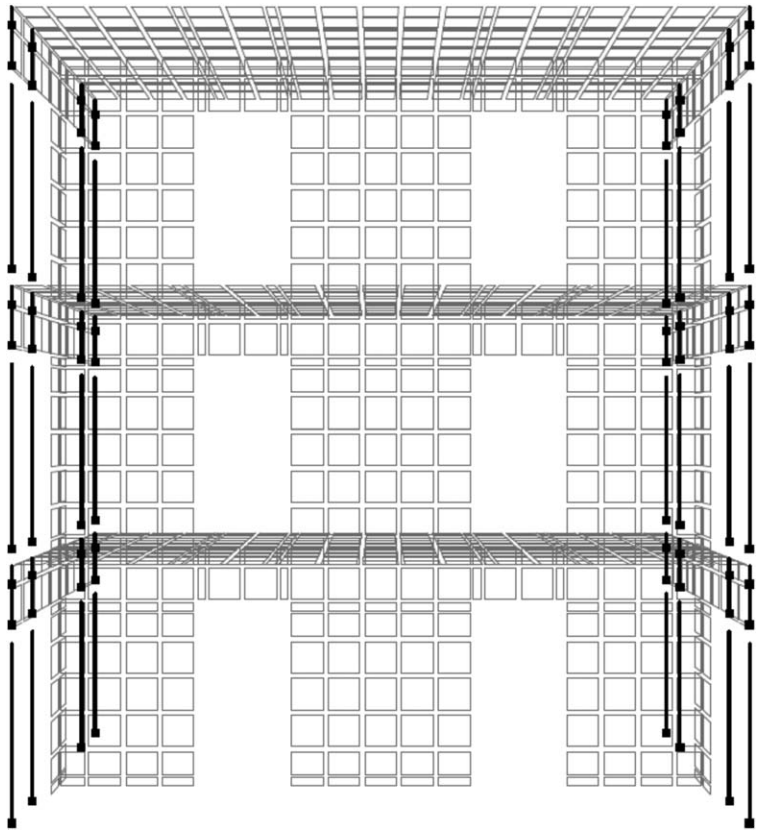

Figure 12. Three-dimensional view of PERFORM-3D model of three-story specimen.

stiffnesses. Effective stiffness values accounting for the effects of flexural cracking were used for the wall and slab elements. To more accurately model the strain demand in potential hinging regions of wall segments, the finite element mesh was refined in those regions using thinner layers for reasons mentioned previously.

A series of ground motion records from the shake-table test were used to conduct nonlinear dynamic analyses. The sequence of input motions, scaling factors, and level of excitation are shown in Table 3. In these nonlinear dynamic analyses, equivalent viscous damping was used to account for energy dissipation in the elastic range, and for this purpose, the assumption of Rayleigh damping was invoked. To account for the effects of accumulated structural degradation on the response of the test building, the selected ground motion records were applied as a sequence of input motions, with 2 s of zero ground acceleration between each to allow the structure to come to rest prior to the next input motion.

Time-history analyses are compared with experimental results for the three-story specimen in terms of three key response parameters: first-floor displacement versus time;

Table 3. Sequence of input motions used for time-history analysis of three-story shake-table specimen

Earthquake	Year	Ground motion	Scaling factor	Level of excitation
Imperial Valley	1979	El Centro	20%	
		El Centro	45%	
		El Centro	90%	
		El Centro	120%	DE
		El Centro	150%	
		El Centro	180%	MCE
		El Centro	250%	Above MCE
Imperial Valley	1940	El Centro#5	300%	
Northridge	1994	Sylmar	125%	MCE
		Sylmar	160%	1.5 MCE

base shear versus time; and load-displacement hysteresis loops. In the interest of space, those comparisons are discussed here for only two ground motions: 250% El Centro 1979 and 160% Sylmar 1994. The input motion of 250% El Centro corresponds to the Maximum Considered Earthquake (MCE). Under 250% El Centro 1979, the first-floor displacement time-history is shown in Figure 13a. Peak displacements are predicted within 10% of the experimental results. In general, agreement between predictions and experiment for first floor lateral displacement is quite good. Predicted base shear was determined by summing the calculated shears at the base of the wall segments, and is shown in Figure 13b. As with displacements, the shear response was well captured, even as the structure degraded. Peak values are within 5% to 10% of the measured values. In general, agreement between prediction and analysis is quite good for a complex structure with significant nonlinearity. Hysteresis loops of base shear versus first-floor displacement are shown in Figure 13c. Because the histories of first-floor displacements and base shears were accurately predicted, it is not surprising that the hysteresis loops also compare well. For 160% Sylmar 1994, which corresponds to about 1.5 times MCE, corresponding displacements, shears, and hysteretic loops of base shear versus first-floor displacement are shown in Figure 14. Because the histories of first-floor displacements and base shears were accurately predicted, the hysteresis loops for this shaking level also compare well. The results show that the General Wall Elements provide a reasonable compromise between ease of modeling, quality of results, and computational effort that can be used for displacement-based seismic design of reinforced masonry shear-wall structures.

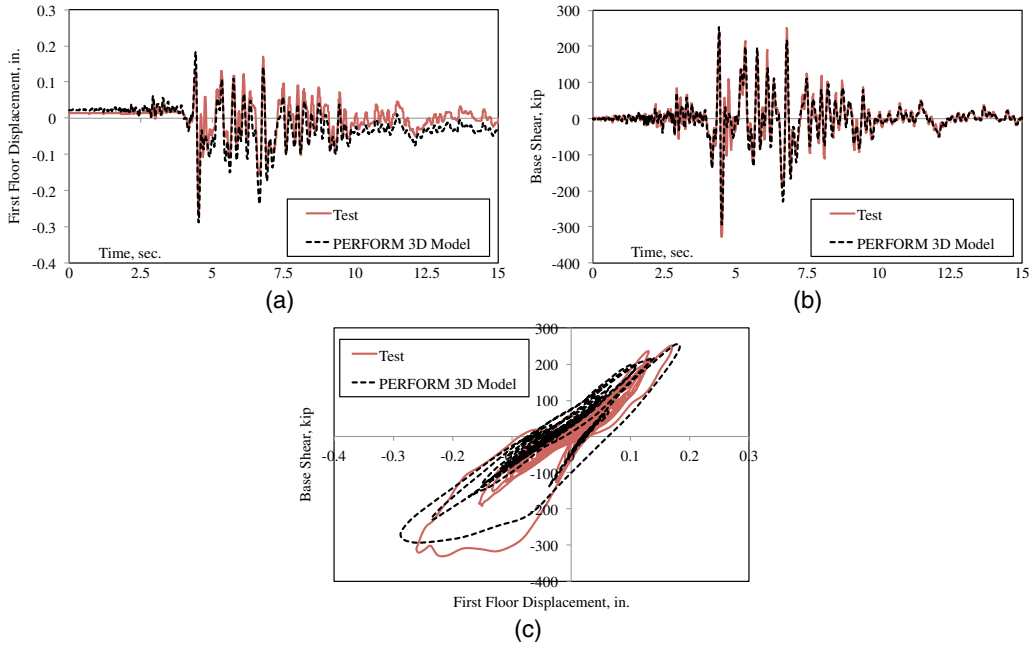

Figure 13. Time-history responses of three-story specimen under 250% El Centro 1979.

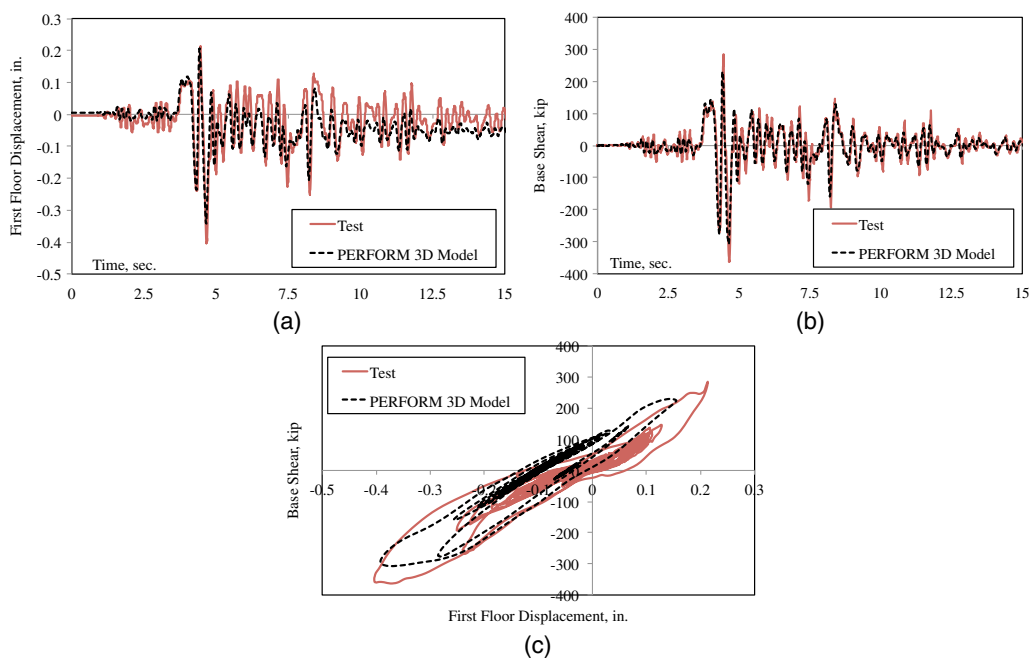

Figure 14. Time-history responses of three-story specimen under 160% Sylmar 1994.

DISPLACEMENT-BASED DESIGN OF TWO-STORY CMU SPECIMEN

OVERALL DESCRIPTION OF FULL-SCALE, TWO-STORY REINFORCED MASONRY SHEAR-WALL STRUCTURE

As a trial application of proposed displacement-based design for reinforced masonry shear walls, a full-scale, two-story, reinforced masonry shear-wall system was developed and designed. Schematic views of the specimen on the shake-table are shown in Figure 15. It had a wall with openings in the direction of shaking. The size and arrangement of openings created wall segments whose behavior was controlled by shear. It had a symmetrical arrangement of wall segments perpendicular to the direction of shaking. As shown in Figure 16, the specimen was rectangular in plan, with out-to-out dimensions of 22.67 ft in the direction of shaking and 20.67 ft perpendicular to the direction of shaking. The wall in the direction of shaking consisted of two T-wall segments (Walls W-1 and W-3) and one lineal wall segment (a wall without flanges, Wall W-2). The walls perpendicular to the direction of shaking were two lineal half-walls. Figure 16 also shows an elevation view of the specimen in the direction of shaking, indicating the locations and the configuration of the openings. As shown in Figure 16, control joints were introduced on each side of the lintel beams above door openings.

In this case, an initial design was produced using the detailing requirements of the limit-design provisions of the draft 2013 MSJC *Code*, including requirements for shear- and flexure-controlled reinforced masonry shear wall elements. In those draft provisions, structural wall segments must have a reinforcement ratio of at least 0.1% in the longitudinal and transverse directions, and the longitudinal and transverse reinforcement must be spaced at the lesser of one-half the longitudinal dimension and one-half the transverse dimension of the segment. For this purpose, Walls W-1 and W-3 were provided with longitudinal reinforcement consisting of No. 4 bars at 16 in. in webs, and two additional No. 4 longitudinal bars in the flanges. Transverse reinforcement consisting of No. 4 horizontal bars at 16 in. was

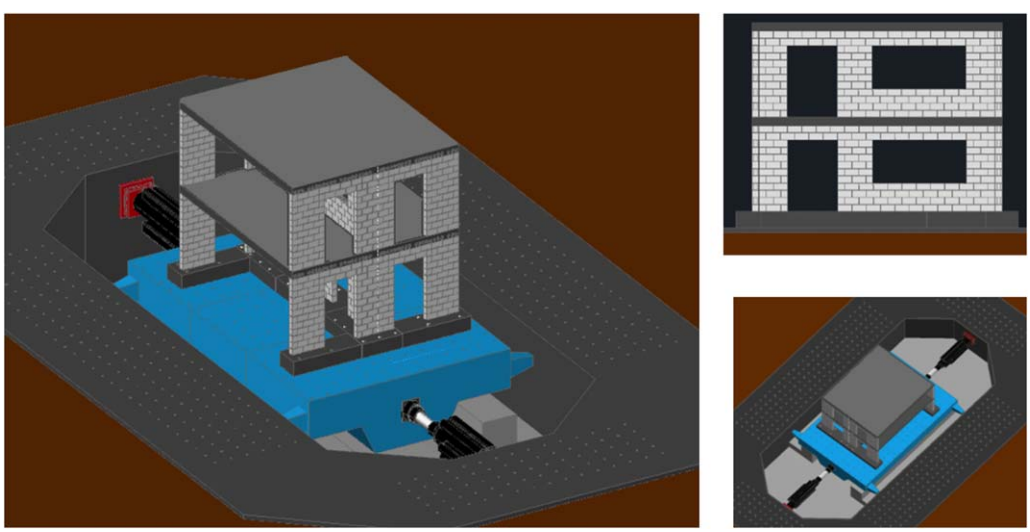

Figure 15. Schematic views of full-scale, two-story specimen on UCSD shake table.

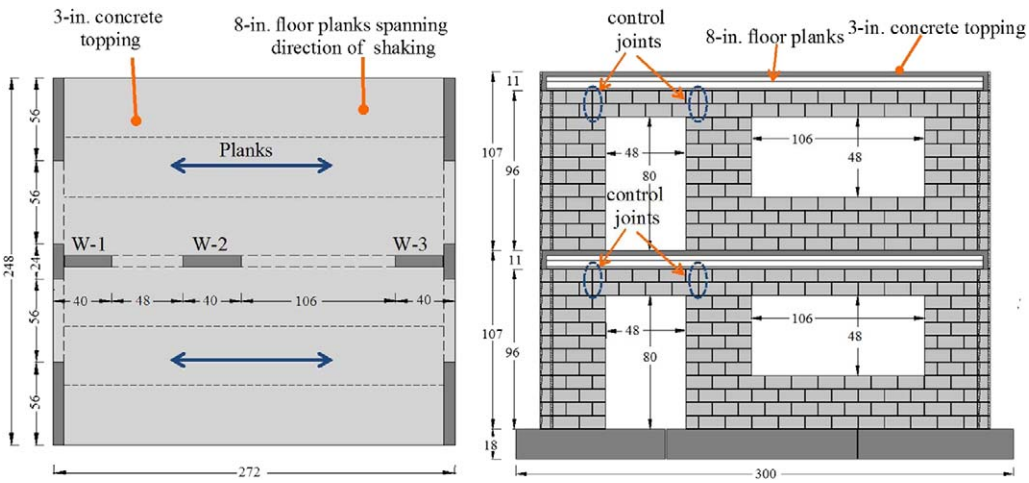

Figure 16. Plan view of typical floor and elevation view of the full-scale, two-story specimen in direction of shaking.

used in the webs and flanges. Wall W-2 was provided with longitudinal reinforcement consisting of No. 4 bars at 16 in., and transverse reinforcement consisting of No. 4 horizontal bars at 16 in. Wall segments W-2 and W-3 were expected to be shear-controlled, while W-1 would be flexure-controlled. The design details are presented in the companion paper (Ahmadi et al. 2013).

DEFINE SEISMIC HAZARDS AND TARGET DRIFTS FOR TWO-STORY SPECIMEN

The risk-targeted Maximum Considered Earthquake level response spectra and the corresponding Design level spectra used for the design (formerly referred to as DBE) were determined according to ASCE/SEI 7 (2010). It was assumed that the structure was to be constructed in a region of high seismicity and was assigned to SDC D, corresponding to $S_S = 1.50$ g, and $S_1 = 0.60$ g, with Site Class D (stiff soil). The spectral displacement values corresponding to the different equivalent hysteretic damping levels of the building, $S_{D-\xi_{eq}}$, can be obtained through empirical modification factors. Figure 17 presents the relative displacement response spectra for different equivalent viscous damping ratios, obtained with Equations 1 and 2.

To assure adequate structural performance for each seismic hazard level, the story drift ratios and local deformation ratios must be checked with the respective target drift limits for the structure. Based on the proposed local deformation ratio limits in Table 1, the flexure-controlled wall segment (Wall W-1) was assigned a maximum local deformation capacity of 0.8% for the DE level and 1.5% for the MCE level, with respect to its clear height. Assuming a fixed-fixed condition, this wall had an effective shear span ratio of 1.0. Shear-controlled wall segments (Walls W-2 and W-3) were assigned a maximum local deformation capacity of 0.5% for the DE level and 1.0% for the MCE level, with respect to their clear heights. Walls W-2 and W-3 (shown in Figure 16) had a clear height that was about 0.5 times the story

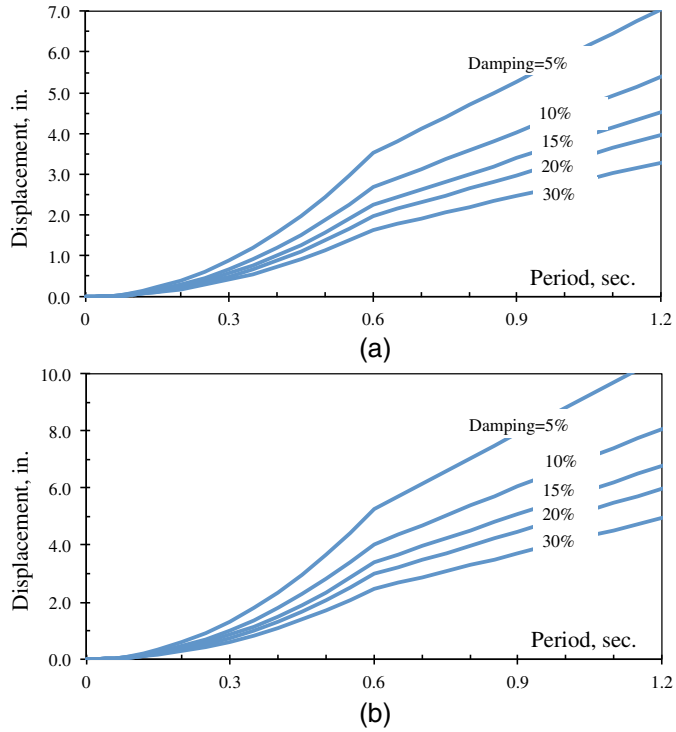

Figure 17. (a) Displacement response spectra for different equivalent damping ratios at DE level and (b) MCE level.

height. For determining the target displacements, the local deformation limits must be translated to story-drift limits. In this consideration, W-2 and W-3 were the most critical walls and controlled the story drifts. Considering that W-2 and W-3 would not be perfectly fixed at their tops and bottoms (because cracks could propagate from window corners into the masonry above and below), the target story drift limits were selected to be 0.3% for DE and 0.6% for MCE.

CONDUCT INELASTIC ANALYSIS AND DETERMINE TARGET DISPLACEMENT LIMITS FOR TWO-STORY SPECIMEN

The nonlinear analytical model was composed of General Wall Elements using PERFORM-3D (CSI 2007). As shown in Figure 18, a non-linear three-dimensional model of the two-story shake-table specimen was developed. The in-plane wall segments (vertical and horizontal) were modeled with the General Wall Elements, permitting in-plane inelastic response anywhere within the perforated multi-story wall. The out-of-plane wall segments were modeled using 3-D inelastic column elements with plastic hinges at each end. The hinges were rigid-plastic, and used a yield surface appropriate for reinforced masonry. The floor slabs were modeled using four-node, elastic shell elements with membrane (in-plane) and plate bending (out-of-plane) stiffnesses. Effective stiffness values

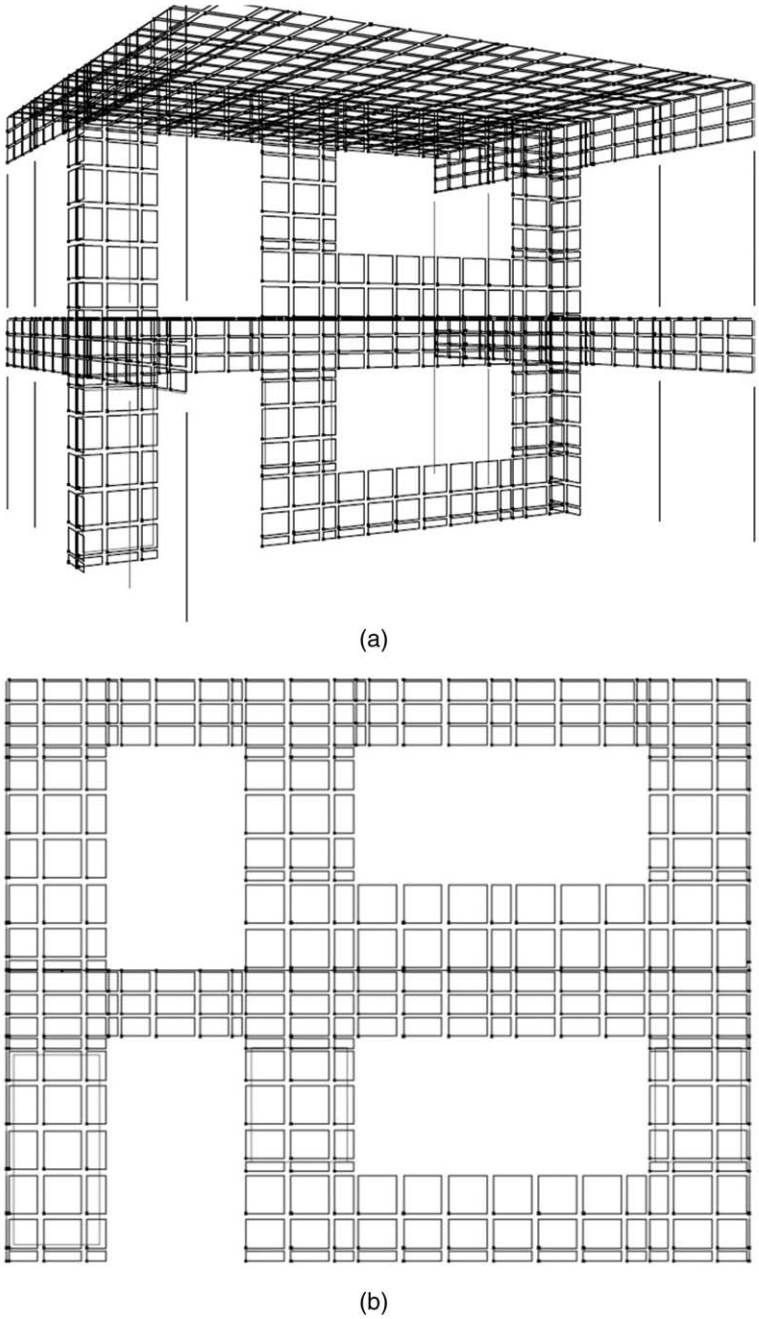

Figure 18. PERFORM-3D model of full-scale, two-story specimen.

including the effects of flexural cracking were used for the elastic components of the wall and slab elements. An effective stiffness of 50% of the gross cross-sectional stiffness was used in the modeling of the wall segments.To better model the regions at the tops and bottoms of vertically oriented wall segments, where plastic hinges were expected to form, 4-in. (10 to 20% of the height of wall) high elements were used there (Ahmadi 2012). A similarly refined mesh was used at the ends of horizontally oriented segments (lintels).

Monotonic pushover analyses were performed to determine the envelope of base shear versus lateral drift ratio and to calculate the expected base shear at the target drift levels. Pushover analysis was conducted using a uniform distribution of load over the height of the structure, applied until the building reached an overall drift ratio of 1.5%. Figure 19 and Figure 20 present the deformed shapes and inelastic mechanisms for DE and MCE levels, and the capacity curve, respectively. The overall displacement shown in Figure 20 is the roof displacement.

To calculate the equivalent target displacement and the effective secant stiffness of the equivalent SDOF system for each hazard level, the deflected shape and global displacements at floor levels obtained from the inelastic pushover analysis were used. These values correspond to the states when the bottom story of the structure reached the drift limits determined for DE and MCE, respectively, as shown in Figure 21.

ESTABLISH EQUIVALENT VISCOUS DAMPING FOR TWO-STORY SPECIMEN

The effective global damping depends on the global displacement and local deformation demands. Using Figure 5, average equivalent hysteretic damping ratios in flexure-dominated Wall W-1 (with an aspect ratio of 1.0) were 16% and 21% at the DE and MCE levels, respectively. The average equivalent hysteretic damping ratios in shear-dominated Walls W-2 and W-3 (with aspect ratio of about 1.0) were 13% and 18% at DE and MCE levels, respectively. Assuming that base shear is distributed among wall segments in proportion to the square of the length of each wall segment (Figure 16), effective global damping ratios for both hazard levels can be calculated by Equation 8.

$$\text{At the DE level: } (\xi_{eq})_{global} = \frac{(40\,\text{in.})^2 \times 0.16 + (40\,\text{in.})^2 \times 0.13 + (40\,\text{in.})^2 \times 0.13}{3(40\,\text{in.})^2} = 0.14$$

$$\text{At the MCE level: } (\xi_{eq})_{global} = \frac{(40\,\text{in.})^2 \times 0.21 + (40\,\text{in.})^2 \times 0.18 + (40\,\text{in.})^2 \times 0.18}{3(40\,\text{in.})^2} = 0.19$$

Hence, equivalent hysteretic damping of 14% is assumed for DE and 19% for MCE.

EQUIVALENT NATURAL PERIOD FOR TWO-STORY SPECIMEN

To determine the required equivalent natural period of the two-story specimen for displacement-based design, the displacement spectra for DE and MCE levels were used, using the equivalent target lateral displacement and the specimen's effective global damping. As discussed in the companion paper (Ahmadi et al. 2013), the tributary seismic mass of the specimen was higher than the actual mass of the specimen. The total seismic weights at the

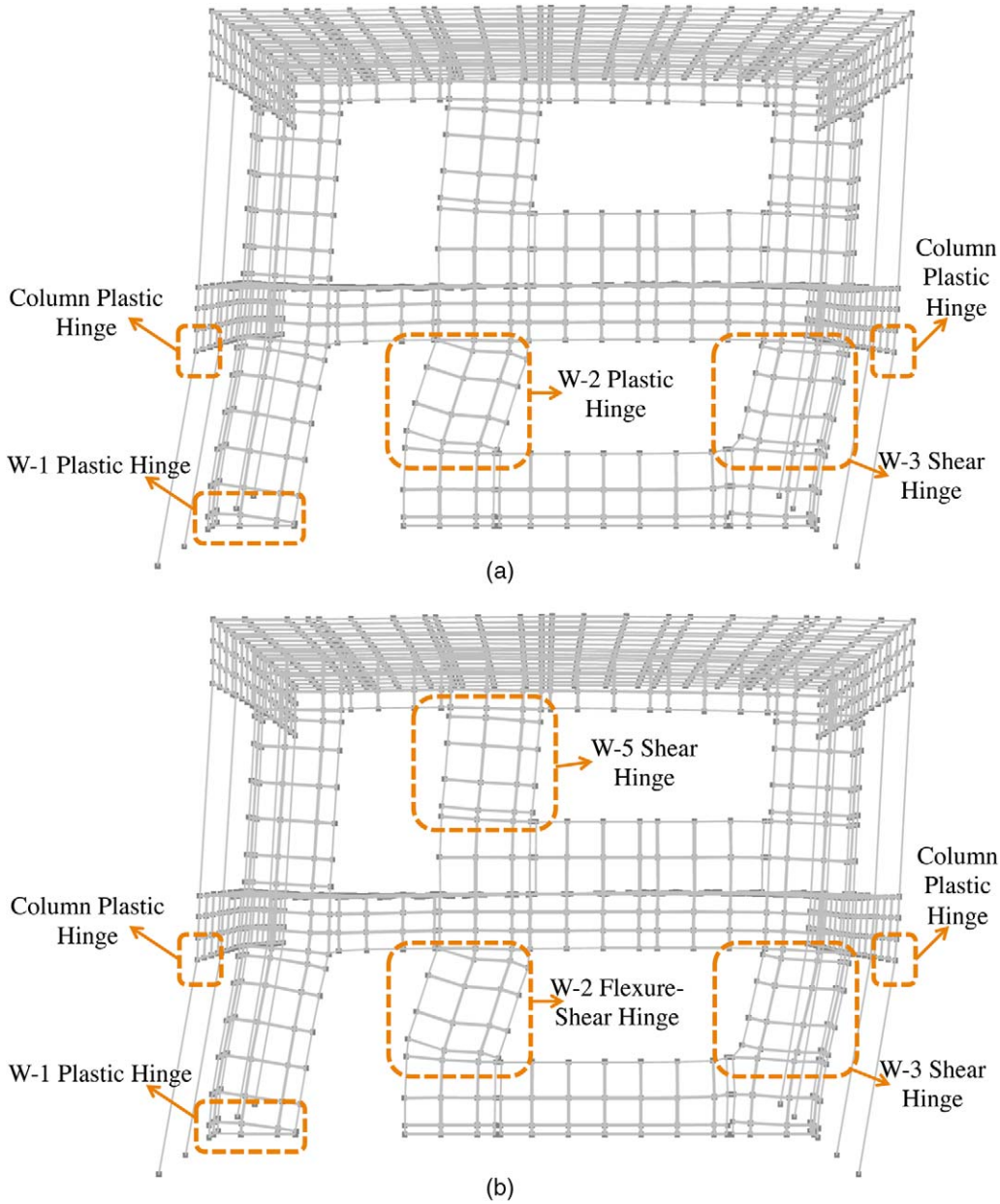

Figure 19. Deflected shapes and inelastic mechanisms from pushover analyses for the two-story specimen in the direction of shaking. (a) Target mechanism at DE (story drift of 0.3%); (b) Target mechanism at MCE (story drift of 0.6%).

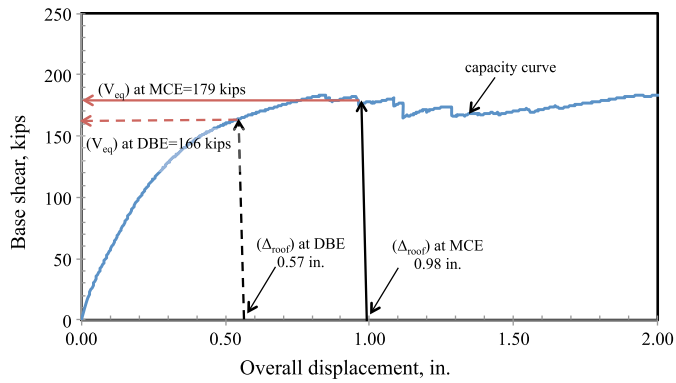

Figure 20. Capacity curve for the full-scale, two-story specimen in direction of shaking and predicted base shear at each hazard level for the two-story specimen.

roof and the first elevated floor were 105.4 and 131.9 kips, respectively. Using Equation 3 and deflected shapes from pushover analysis (Figure 21), the equivalent target lateral displacement for each hazard level can be calculated:

$$(\Delta_{eq})_{DE} = \frac{105.4\,\text{kip} \times (0.57\,\text{in.})^2 + 131.9\,\text{kip} \times (0.31\,\text{in.})^2}{105.4\,\text{kip} \times 0.57\,\text{in.} + 131.9\,\text{kip} \times 0.31\,\text{in.}} = 0.47\,\text{in.}$$

$$(\Delta_{eq})_{MCE} = \frac{105.4\,\text{kip} \times (0.98\,\text{in.})^2 + 131.9\,\text{kip} \times (0.62\,\text{in.})^2}{105.4\,\text{kip} \times 0.98\,\text{in.} + 131.9\,\text{kip} \times 0.62\,\text{in.}} = 0.83\,\text{in.}$$

Using the DE response spectrum for 14% damping, the required equivalent natural period can be obtained for this hazard level. As shown in Figure 22a, using the DE response spectrum for 14% damping, the equivalent displacement of 0.47 in. corresponds to an equivalent natural period of 0.27 s As shown in Figure 22b, using the MCE response spectrum for 19% damping, the equivalent displacement of 0.83 in. corresponds to an equivalent natural period of 0.32 s.

REQUIRED BASE SHEAR FOR TWO-STORY SPECIMEN

The required equivalent lateral stiffness, $(k_{eq})_{req.}$ and the required base shear can be obtained using the equivalent natural periods calculated in the previous step, the specimen's target equivalent lateral displacement, and the effective seismic weight. Using Equation 4, the effective seismic weight for each hazard level can be calculated:

$$(W_{eff})_{DE} = \frac{(105.4\,\text{kip} \times 0.57\,\text{in.} + 131.9\,\text{kip} \times 0.31\,\text{in.})^2}{105.4\,\text{kip} \times (0.57\,\text{in.})^2 + 131.9\,\text{kip} \times (0.31\,\text{in.})^2} = 218\,\text{kip}$$

$$(W_{eff})_{MCE} = \frac{(105.4\,\text{kip} \times 0.98\,\text{in.} + 131.9\,\text{kip} \times 0.62\,\text{in.})^2}{105.4\,\text{kip} \times (0.98\,\text{in.})^2 + 131.9\,\text{kip} \times (0.62\,\text{in.})^2} = 226\,\text{kip}$$

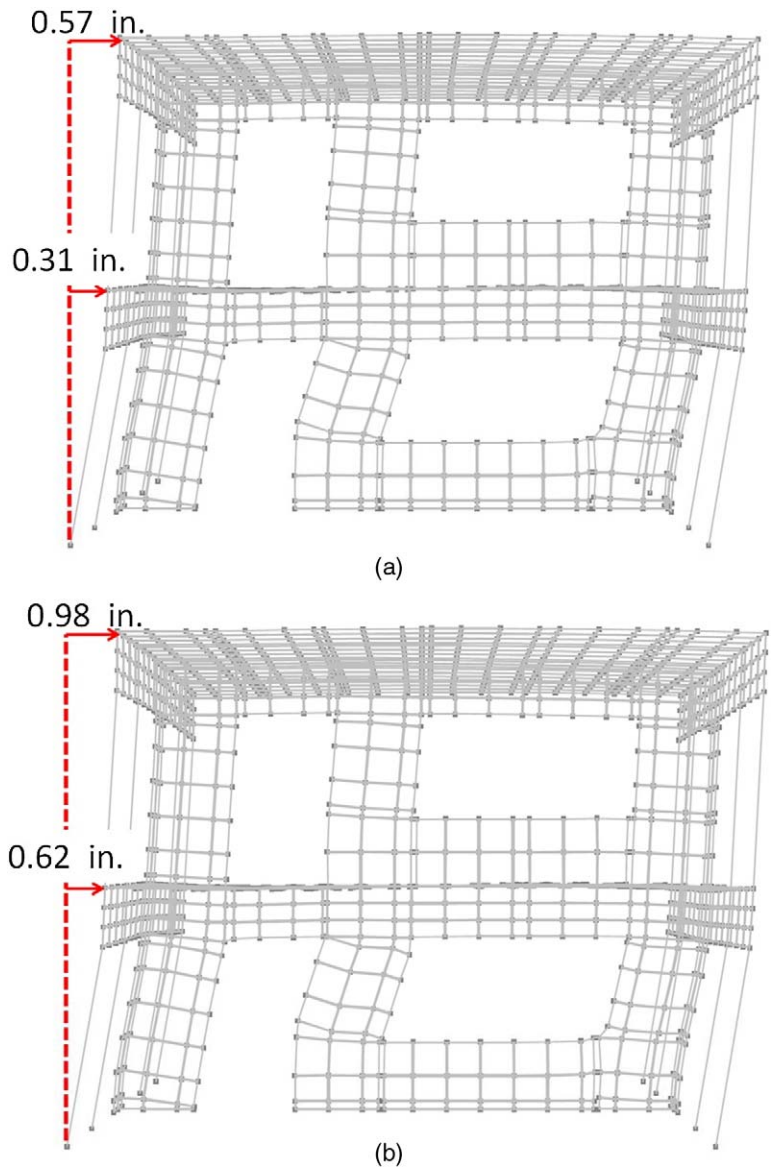

Figure 21. (a) Overall displacement at target drift of 0.3% for DE, and (b) Overall displacement at target drift of 0.6% for MCE.

The required equivalent lateral stiffness and the required base shear for each hazard level can then be calculated using Equations 8 and 9. As calculated below, for the DE level, the required stiffness is 306 kip/in., and the required base shear is 144 kips:

$$((k_{eq})_{req})_{DE} = \frac{4\pi^2 W_{eff}}{gT_{eq}^2} = \frac{4\pi^2 \times 218\,\text{kip}}{g \times (0.27\ \text{sec.})^2} = 306\,\text{kip/in.}$$

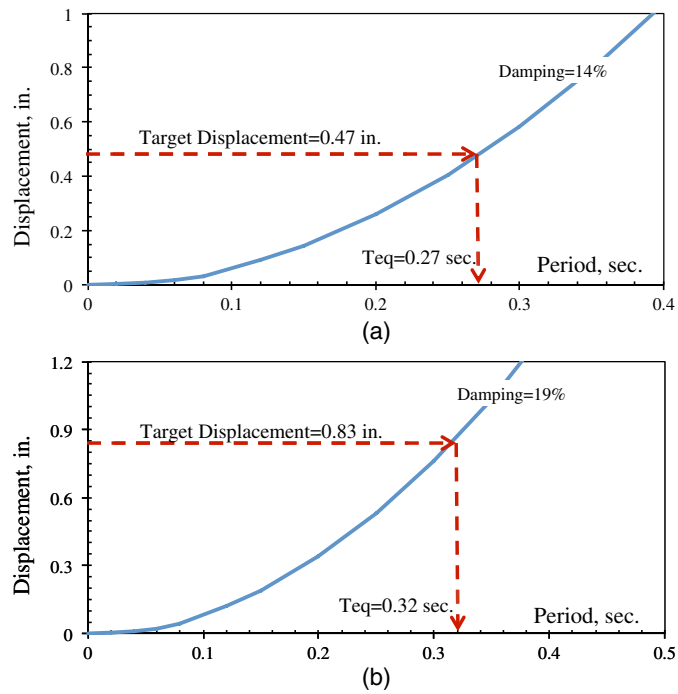

Figure 22. (a) Equivalent natural period of two-story specimen at DE; (b) equivalent natural period of two-story specimen at MCE.

$$(V_{req})_{DE} = ((k_{eq})_{req})_{DBE} \times \Delta_{eq-DBE} = 308\,\text{kip/in.} \times 0.47\,\text{in.} = 144\,\text{kip}$$

For the MCE level, the required stiffness is 225 kip/in., and the required base shear is 186 kips.

$$((k_{eq})_{req})_{MCE} = \frac{4\pi^2 W_{eff}}{gT_{eq}^2} = \frac{4\pi^2 \times 226\,\text{kip}}{g \times (0.32\ \text{sec.})^2} = 225\,\text{kip/in.}$$

$$(V_{req})_{MCE} = ((k_{eq})_{req})_{MCE} \times \Delta_{eq-MCE} = 225\,\text{kip/in.} \times 0.83\,\text{in.} = 186\,\text{kip}$$

VERIFY BASE SHEAR FOR TWO-STORY SPECIMEN

In this step, the capacity curve from a static pushover analysis, shown in Figure 20, and the target displacements at the roof level were used to obtain the base-shear capacities that would be developed by the structure at DE and MCE levels. At DE hazard level, using the overall roof displacement of 0.57 in., the capacity curve gives a base shear of 166 kip; and at MCE hazard level, using the overall roof displacement of 0.98 in., the base shear is 179 kip. The base-shear capacities from the pushover curve were compared to the required base shears

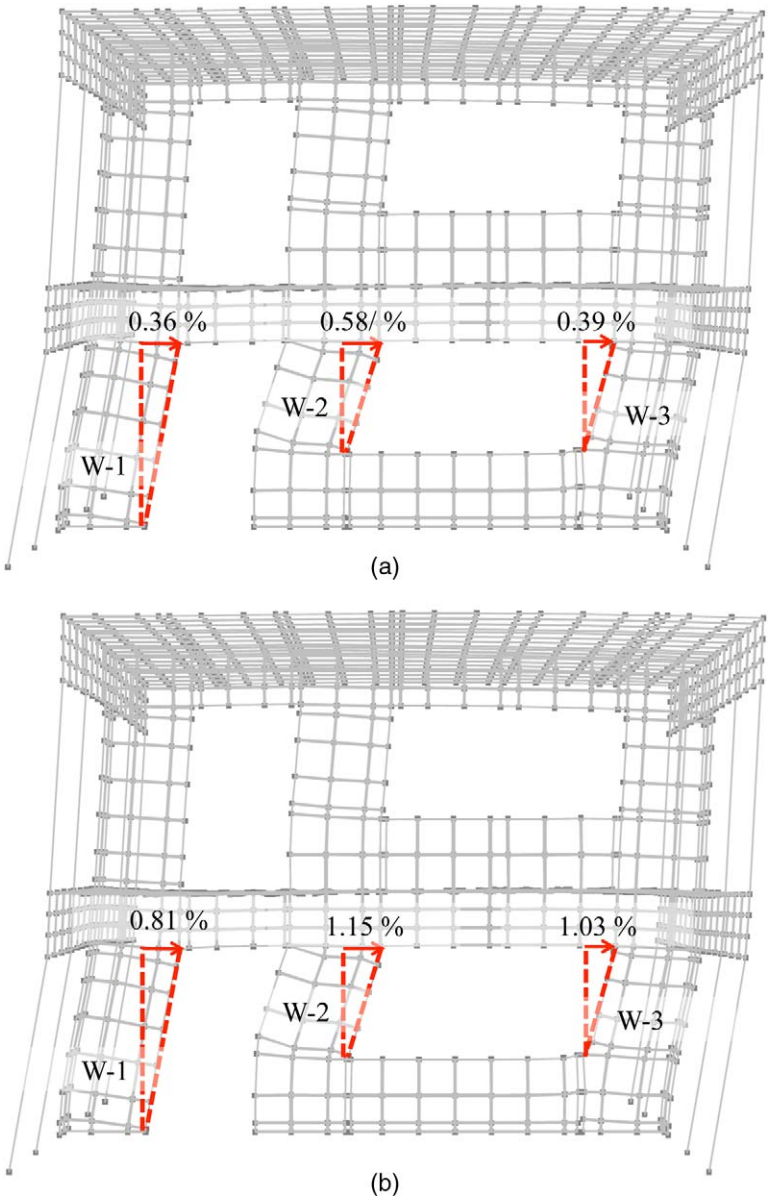

Figure 23. Local deformation demands in wall segments of two-story specimen. (a) Local deformation demands at DE; (b) Local deformation demands at MCE.

for each hazard level. At DE level, the base-shear capacity and the required base shears were close. At MCE level, the base-shear capacity was slightly less than the required base shear. However, the design was not further refined at this stage. As discussed in the companion paper (Ahmadi et al. 2015) on verification, the design was later checked using nonlinear time-history analysis and was judged satisfactory for the ground motions selected for testing.

FINAL DESIGN OF THE FULL-SCALE, TWO-STORY SPECIMEN

Figure 23 shows the maximum deformation demands in Walls W-1, W-2, and W-3 at the ground level, under DE- and MCE-level motions, calculated in the pushover analysis described previously. As shown in the figure, the deformation demand on Wall W-2 was 0.58% at DE and 1.15% at MCE level. These local deformation demands slightly exceeded the expected deformation capacities for shear-controlled wall elements. This was considered acceptable because the top and bottom ends of the wall components were not completely fixed, while the deformation limits were based on fixed-based end conditions. In fact, this situation was accounted for in the target story-drift limits.

The displacement-based design and the associated analysis showed that the preliminary design based on the limit-design requirements of the draft 2013 MSJC *Code* was adequate. Therefore, no revision was made. However, this design did not meet requirements for prescriptive reinforcement in the body of the 2011 MSJC *Code* for "special" reinforced masonry shear walls. Wall W-2 and the webs of Walls W-1 and W-3 had flexural reinforcement consisting of No. 4 bars at 16 in. All the walls had No. 4 horizontal bars at 16 in. for transverse reinforcement. The prescriptive requirements of the 2011 MSJC *Code* would require a maximum bar spacing of no more than 13 in. for both longitudinal and transervse reinforcement.

SUMMARY AND CONCLUSIONS

In this paper, specific guidelines and analytical tools have been developed for displacement-based design of reinforced masonry wall systems. The procedure anticipates the formation of a plastic mechanism, calculates the deformation demands associated with that mechanism, and ensures that those deformation demands remain below acceptable deformation limits for flexure-dominated and shear-dominated wall segments. Nonlinear analytical models for masonry shear-wall structures were developed and calibrated using results from full-scale, wall specimens tested with quasi-static cyclic loads, and were validated using shake-table tests of a full-scale, three-story specimen designed using the conventional force-based procedure. The validated nonlinear analytical models provided a reasonable compromise between ease of modeling, quality of results, and computational effort for the displacement-based design method. The displacement-based design method was used to design a full-scale, two-story reinforced masonry wall system with shear-critical wall components, which was evaluated with shake-table tests, as discussed in a companion paper. The procedure is more consistent and transparent than current force-based seismic design procedures, and it is suitable for use by experienced design offices. For future studies, the displacement-based design method can be extended to low-rise reinforced masonry structures with deformable roof or floor diaphragms.

REFERENCES

Ahmadi, F., 2012. Displacement-based Seismic Design and Tools for Reinforced Masonry Shear-Wall Structures, Ph.D. Thesis, The University of Texas at Austin.

Ahmadi, F., Mavros, M., Klingner, R. E., Shing, B., and McLean, D., 2015. Displacement-based seismic design for reinforced masonry shear-wall structures, part 2: Validation with shake-table tests, *Earthquake Spectra* **31**, 999–1019.

American Society of Civil Engineers (ASCE), 2010. ASCE/SEI 7-10: *Minimum Design Loads for Buildings and Other Structures*, American Society of Civil Engineers, Reston, VA.

Borzi, B., and Elnashai, A. S., 2000. *Refined force reduction factors for seismic design, Journal of Engineering Structure* **22**, 1244–1260.

Calvi, G., and Kingsley, G. R., 1995. Displacement-based seismic design of multi-degree-of-freedom bridge structures, *Earthquake Engng. Struct. Dyn.* **24**, 1247–1266.

Calvi, G., 1999. A displacement-based approach for vulnerability evaluation of classes of buildings, *Journal of Earthquake Engineering* **3**, 411–438.

Computers & Structures, Inc. (CSI), 2007. *PERFORM-3D V5, Nonlinear Analysis and Performance Assessment for 3D Structures*, Computer and Structures, Inc., Berkeley, CA.

European Committee for Standardization (CEN), 1998. *Eurocode 8: Design Provisions for Earthquake Resistance of Structures, Part 1-1, 1-2 and 1-3*, European Pre-standard ENV 1998-1-1, 1-2, and 1-3, Brussels.

Filiatrault, A., and Folz, B., 2002. Performance-Based Seismic Design of Wood Framed Buildings, *Journal of Structural Engineering*, ASCE **128**, 39–47.

Klingner, R. E., 1994. *Performance of Masonry Structures in the Northridge, California Earthquake of January 17, 1994*, Technical Report 301-94, The Masonry Society, Boulder, CO, 100 pp.

Masonry Standards Joint Committee (MSJC), 2011. *Building Code Requirements for Masonry Structures* (TMS 402-11/ACI 530-11/ASCE 5-11), The Masonry Society, Boulder, CO; American Concrete Institute, Farmington Hills, MI; and American Society of Civil Engineers, Reston, VA.

Masonry Standards Joint Committee (MSJC), 2013. *Building Code Requirements for Masonry Structures* (TMS 402-13/ACI 530-13/ASCE 5-13), The Masonry Society, Boulder, CO; American Concrete Institute, Farmington Hills, MI; and American Society of Civil Engineers, Reston, VA.

Mehrabi, A. B., and Shing, P. B., 2003. Seismic analysis of masonry-infilled reinforced concrete frames, *The Masonry Society Journal*, 9–22.

Miranda, E., and Bertero, V. V., 1994. Evaluation of strength reduction factor for earthquake-resistance design, *Earthquake Spectra* **10**, 357–379.

Moehle, J. P., 1992. Displacement-based design of RC structures subjected to earthquakes, *Earthquake Spectra* **8**, 403–428.

Munshi, J. A., and Ghosh, S. K., 2000. Displacement-based seismic design of coupled shear wall systems, *Earthquake Spectra* **16**, 621–642.

Priestley, M. J. N, 1997. Displacement-based seismic assessment of reinforced concrete buildings, *Journal of Earthquake Engineering* **1**, 157–192.

Priestley, M. J. N., Calvi, G. M., and Kowalsky, M. J., 2007. *Direct Displacement-Based Seismic Design of Structures*, IUSS, University of Pavia, Pavia, Italy.

Sherman, J. D., 2011. Effects of Key Parameters on the Performance of Concrete Masonry Shear Walls Under In-Plane Loading, M.S. Thesis, Washington State University, Pullman, WA.

Stavridis, A., Ahmadi, F., Mavros, M., Shing, P., Klingner, R. E., and McLean, D., 2012. Shake-table testing of a three-story, full-scale reinforced masonry wall system, in *The 15th International Brick and Block Masonry Conference*, Brazil.

Sullivan, T. J., Priestley, M. J. N., and Calvi, G. M., 2006. Direct displacement-based design of frame-wall structures, *Jounal of Earthquake Eng* **10**, 91–124.

(Received 2 December 2012; accepted 5 July 2013)